Article

J. Biol. Regul. Homeost. Agents. 2024; 38(5): 4185–4196
https://doi.org/10.23812/j.biol.regul.homeost.agents.20243805.332

Resveratrol Exerts Inhibitory Effects on the Growth and Metastasis of Lung Cancer and Modulates the Polarization of Tumor-Associated Neutrophils

Guanbiao Liang[1], Huajian Peng[1], Shuyu Lu[1], Yongpeng Li[1], Nuo Yang[1,*]

[1]Department of Cardiothoracic Surgery, The First Affiliated Hospital of Guangxi Medical University, 530000 Nanning, Guangxi, China
*Correspondence: yangnuo@gxmu.edu.cn (Nuo Yang)
Published: 1 May 2024

Background: The resveratrol (RES) exhibits inhibitory effects against lung cancer through various targets. However, the exact underlying mechanism remains unclear. This study aims to investigate the effect of RES on the growth and metastasis of lung cancer and its impact on polarization of tumor-associated neutrophils (TANs) and epithelial-mesenchymal transition (EMT).
Method: The A549 lung cancer cell line was treated with varying concentrations (0, 5, 10, 20, 40, and 60 μM) of RES. The impact of RES on cellular proliferation was assessed using Cell Counting Kit-8 (CCK-8) assay, and the optimal dosage was selected for subsequent analysis. Furthermore, the effects of RES treatment on the apoptosis, invasion, and migration of the cells, along with its impact on the EMT process, were examined. Neutrophils were isolated from the blood of the health individuals and were co-cultured with A549 cells to investigate the TANs polarization. Additionally, we established a nude mouse model of the subcutaneous tumor. The lung cancer growth, tumor tissue pathology, and tumor cell metastasis were evaluated.
Results: We observed that RES effectively suppressed A549 cell growth in a concentration-dependent manner within the dosage range of 10–40 μM ($p < 0.001$). Furthermore, RES promoted A549 cell apoptosis while limiting invasion and migration ($p < 0.001$). Moreover, RES was observed to regulate the EMT pathway in A549 cells, thereby limiting its progression ($p < 0.01$). Notably, RES restricted lung cancer by inducing TANs to polarize toward type N1 while impeding type N2 polarization ($p < 0.001$). In the nude mouse model, RES demonstrated the above-mentioned effects and considerably reduced lung cancer growth, improved tumor tissue pathology, and limited tumor growth ($p < 0.01$), as well as reduced the expression of Matrix Metalloproteinase-2 (MMP2) and MMP9 ($p < 0.05$).
Conclusion: Overall, RES effectively reduces lung cancer growth and tumor cell metastasis by boosting N1 polarization of TAN, suppressing N2 polarization, and reducing EMT.

Keywords: resveratrol; EMT; TAN polarization; lung cancer

Introduction

Lung cancer, one of the most prevalent types of malignancies, offers substantial challenges in treatment because of its ability to spread extensively and the formation of distant metastases. Resveratrol (RES), a polyphenolic compound, has drawn attention in cancer research due to its significant antioxidant, anti-inflammatory, and anti-cancer properties. A study conducted by Zhang *et al.* [1] identified that RES (10 mg/kg) effectively inhibits the development of colon cancer by activating the ROS-dependent ferroptosis pathway. Another study found that oral administration of RES (20 mg/kg) is linked with increased oxidative activity, decreased glycolysis, and reduced lactate production at the sites of ovarian cancer, potentially helping in restoring anti-tumor immunity [2]. Xie *et al.* [3] suggested that RES (120 mg/kg) exerts inhibitory effects on lung cancer growth by modulating tumor microenvironment (TME), explicitly targeting Interleukin-6 (IL-6) and Wnt/β-catenin signaling pathway. Previous research has indicated the efficacy of resveratrol in suppressing various cancer cell lines, including those associated with lung cancer.

Furthermore, additional study conducted on mice with mammary tumors has demonstrated that RES can affect specific immune cells, such as T cells, tumor-associated neutrophils (TANs), and tumor-associated macrophages (TAMs) within the TME. These effects can stimulate immunological activation, thereby boosting anti-tumor immunity [4]. TANs, a subgroup of neutrophils and a significant component of the TME, are recognized for their role in modulating immunological responses and promoting tumor progression [5]. Hu Q *et al.* [6] performed a single-cell transcriptomic analysis on patients with non-small cell lung cancer (NSCLC) utilizing a publicly available database. They indicated that pro-tumor TAN clusters, characterized by elevated expression of HMGB1, could serve as indicators for clinical outcomes and efficacy of immunotherapy in NSCLC. External stimulation of the TME may prompt

Journal of
BIOLOGICAL REGULATORS
and Homeostatic Agents

the accumulation of TAN in the locoregional area and transition between anti-tumor and pro-tumor phenotypes, i.e., the polarized state of TANs (N1 and N2 types) [5]. The presence of N1 TANs leads to the establishment of an immunological response to the tumor, thereby restricting the development of the tumor, but the presence of N2 TANs may be involved with phenomena such as tumor evasion of immune surveillance and resistance to therapy [7]. Chung JY *et al*. [8] found that reducing the expression levels of *SMAD3* may improve the anticancer properties of neutrophils against NSCLC by improving the maturation of N1 TANs. Consequently, modulating the polarization state of TANs might be a novel strategy to intervene in the progression of lung cancer [8]. In summary, TANs play a crucial role in the development of lung cancer, whereas RES exhibits anti-tumor properties by regulating the TME in lung cancer. Additionally, studies have shown that RES may also regulate TAN in breast cancer. Therefore, we postulated that RES might potentially modulate the polarization of TAN, thereby exerting anti-lung cancer effects.

This study aims to thoroughly investigate the therapeutic effects of RES in lung cancer and its underlying molecular mechanism, focusing on its regulatory impacts on TANs. Utilizing a systematic experimental design, we intend to elucidate the mechanism of action of RES in the growth and metastasis of lung cancer and to interpret its effects on the polarization state of TANs. This study will help enhance our understanding of the role of RES in the treatment of lung cancer. It will also provide a theoretical and experimental basis for developing more effective and innovative anti-lung cancer treatment strategies. Considering the significant challenges in developing effective lung cancer therapy, this research offers promising clinical applicability. By investigating this novel therapeutic strategy, we expect to optimize the prognosis and treatment outcomes for patients with lung cancer.

Materials and Methods

The Extraction of Neutrophils

A peripheral blood sample was obtained from a healthy individual and diluted with phosphate-buffered saline (PBS) before being carefully added to the upper layer of the human peripheral blood lymphocyte separation solution (C0025, Beyotime, Shanghai, China). The sample was then centrifuged at 1200 ×g for 25 minutes, and the supernatant was removed. The red blood cell lysate was then added to resuspend the cells at a volume ratio of 3:1 and incubated on ice for 30 minutes. After centrifugation at 400 ×g, the supernatant was carefully discarded, and the cell pellet was re-suspended in PBS. This process was repeated with another centrifugation at 400 ×g, discarding the supernatant to leave behind the neutrophil pellet.

All the study participants provided written informed consent, and the study protocol adhered to the principles outlined in the Declaration of Helsinki. Furthermore, the study design was approved by the ethics committee of the First Affiliated Hospital of Guangxi Medical University, China (GXMU2023010). The isolated neutrophils underwent mycoplasma testing, and no mycoplasma infection was found. Finally, the viability of neutrophils was verified using flow cytometry analysis.

Cell Culture and Treatment

A549 lung cancer cells (CL-0016, Pricella, Wuhan, China) were cultivated in Dulbecco's Modified Eagle Medium (DMEM) supplemented with 10% fetal bovine serum (FBS) (MBS555798, MyBioSource, San Diego, CA, USA), penicillin (100 U/mL, B21110, R&D Systems, Minneapolis, MN, USA), and streptomycin (100 g/L, B21110, R&D Systems, Minneapolis, MN, USA) and incubated at 37 °C and 5% CO_2. The cells were then passaged using 0.25 percent trypsin-EDTA (MBS2564393, MyBioSource, San Diego, CA, USA) digestion. For all the following experiments, the cells at their logarithmic growth phase were collected. The cells were randomly categorized into three groups, where each group received a different RES (R408711, Aladdin, Shanghai, China) treatment. These groups included the control group (no RES treatment), the 20 μM RES group, and the 40 μM RES group.

Co-culture system: The Transwell insert was utilized to establish a co-culture system of TAN cells and A549 cells. The experiment was divided into three groups. A Control group, where A549 cells were cultured under standard growth conditions; a Model group, in which A549 cells were placed at the lower chamber of the Transwell inserts, while TAN cells were placed at the upper chamber of the Transwell inserts; and a RES group, in which both the A549 cells and RES (40 μM) were positioned at the lower chamber, whereas, the TAN cells were placed at the upper chamber of the Transwell insert. Following a 24-hour incubation, A549 cells were isolated from all the experimental groups and were utilized for further experimentation.

All the cells utilized in the experiment were STR-identified and mycoplasma-tested.

Cell Counting Kit-8 (CCK-8)

A549 cells were categorized into distinct groups based on the treatment with varying concentrations of RES (0, 5, 10, 20, 40, and 60 μM). Following RES treatment, the cells were subsequently cultured, and their proliferative capabilities were assessed using the CCK-8 assay. For this assay, a CCK-8 reagent (C0037, Beyotime, Shanghai, China) was added to each well containing the cells. After thorough mixing, the cells were incubated, and the optical density (OD) at 450 nm was calculated using an enzyme-linked immunosorbent assay (ELISA) reader.

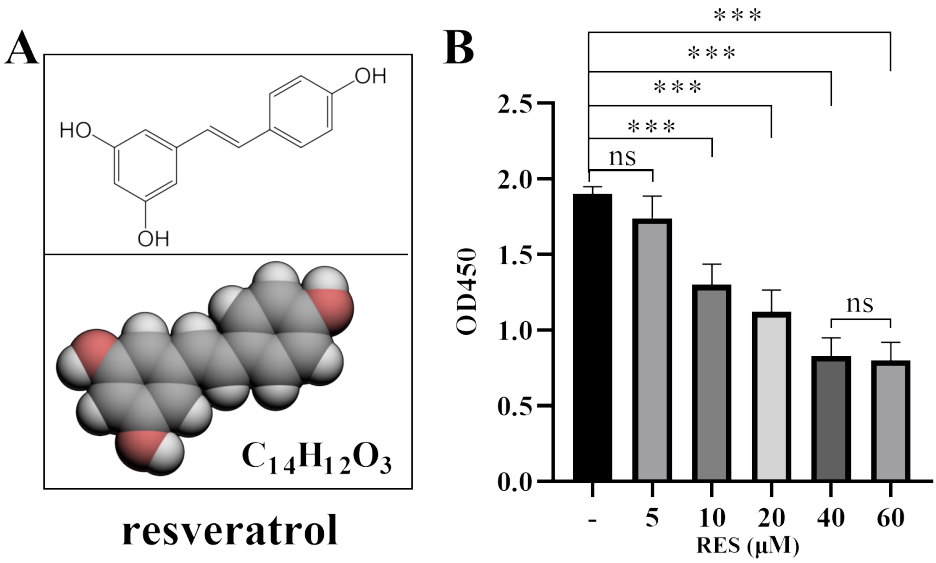

Fig. 1. Effects of resveratrol (RES) dosages on the proliferation of A549 cells. (A) The structure of RES. (B) Impact of varying concentrations of RES (0, 5, 10, 20, 40, and 60 μM) on A549 cell proliferation (n = 3). *** means $p < 0.001$, and *ns* means no statistical difference. The findings were expressed as the mean ± standard deviation (SD).

Transwell and Scratch Experiments

Transwell assay: A complete medium (500 μL) was added to the lower chamber of a Transwell insert (CLS3422, Merck, Darmstadt, Germany). After 48 hours, A549 cells, which were in the logarithmic growth phase, were seeded into the upper chamber of the Transwell inserts at a density of 2.5×10^5 cells/mL. Before the experiments, the chamber was precoated with Matrigel gel (356255, Corning Life Sciences, Corning, NY, USA) at a volume of 100 μL per well. To fix the cells, they were treated with 4% paraformaldehyde at room temperature for ten minutes. The cell invasion rate was determined by counting the number of invaded cells using microscopy after performing hematoxylin and eosin (H&E) staining.

Scratch assay: A549 cells were seeded in a 6-well plate as a single-cell suspension. Once the cells successfully adhered to the walls of the wells, a vertical incision was made along the line on the well's back using a 200 μL pipette tip (EA-007, Creative BioMart, Shirley, NY, USA). After washing with PBS, cells were cultivated in the serum-free medium. Finally, the healing of scratches was observed and noted using a microscope (CX43, Olympus, Tokyo, Japan), and images were captured using a camera at 0- and 48-hour post-scratching period.

Flow Cytometry

Co-cultured cells were seeded into 24-well plates. The medium was aspirated, and the cells were digested, cultured, and rinsed twice. Following the instructions provided by AnnexinV-FITC/PI kit (MBS2557014, MyBioSource, San Diego, CA, USA), the cells were collected, the binding solution was added, and they were suspended through gently pipetting. Subsequently, 10 μL of Annexin V-FITC (MBS668896, MyBioSource, San Diego, CA, USA) was added, and the cells were incubated. In the next step, 5 μL of PI (MBS668896, MyBioSource, San Diego, CA, USA) was added, followed by incubation. Finally, the apoptosis rate was assessed by flow cytometry.

To determine the proportion of Inducible Nitric Oxide Synthase (iNOS)/Cluster of Differentiation (CD)206^+ $CD16b^+$ labeled neutrophils in each group, 1 mL of neutrophil suspension was transferred to a sterile centrifuge tube and centrifuged at 1500 r/min for 10 min. After discarding the supernatant, the cells were resuspended in PBS. After this, 1 μL FC Block (564765, Becton Dickinson and Company, Franklin Lakes, NJ, USA) was added, and the mixture was incubated. In the next step, 1 μL of APC-labeled iNOS (ab115819, abcam, Shanghai, China) or CD206 (E-AB-F1161C, Elabscience, Wuhan, China) antibody was added sequentially, along with PE-labeled CD16b antibody (FHB05710, AntibodySystem, Strasbourg, France). The samples were protected from light, washed, resuspended, and analyzed utilizing flow cytometry to determine the proportion of iNOS/$CD206^+$ $CD16b^+$ labeled neutrophils.

Animals and Model

All experimental procedures involving animals were approved by the Animal Experimentation Ethics Committee of the First Affiliated Hospital of Guangxi Medical University, China (GXMUD2023008). Male BALB/CA nude mice aged 8–10 weeks (20 ± 1 g, Vital River) were housed in an SPF-grade environment. A549 cells (5×10^6/200 μL) were subcutaneously injected into the right side of the nude mouse. After seven days of the injection, an obvious lump

Journal of
BIOLOGICAL REGULATORS
and Homeostatic Agents

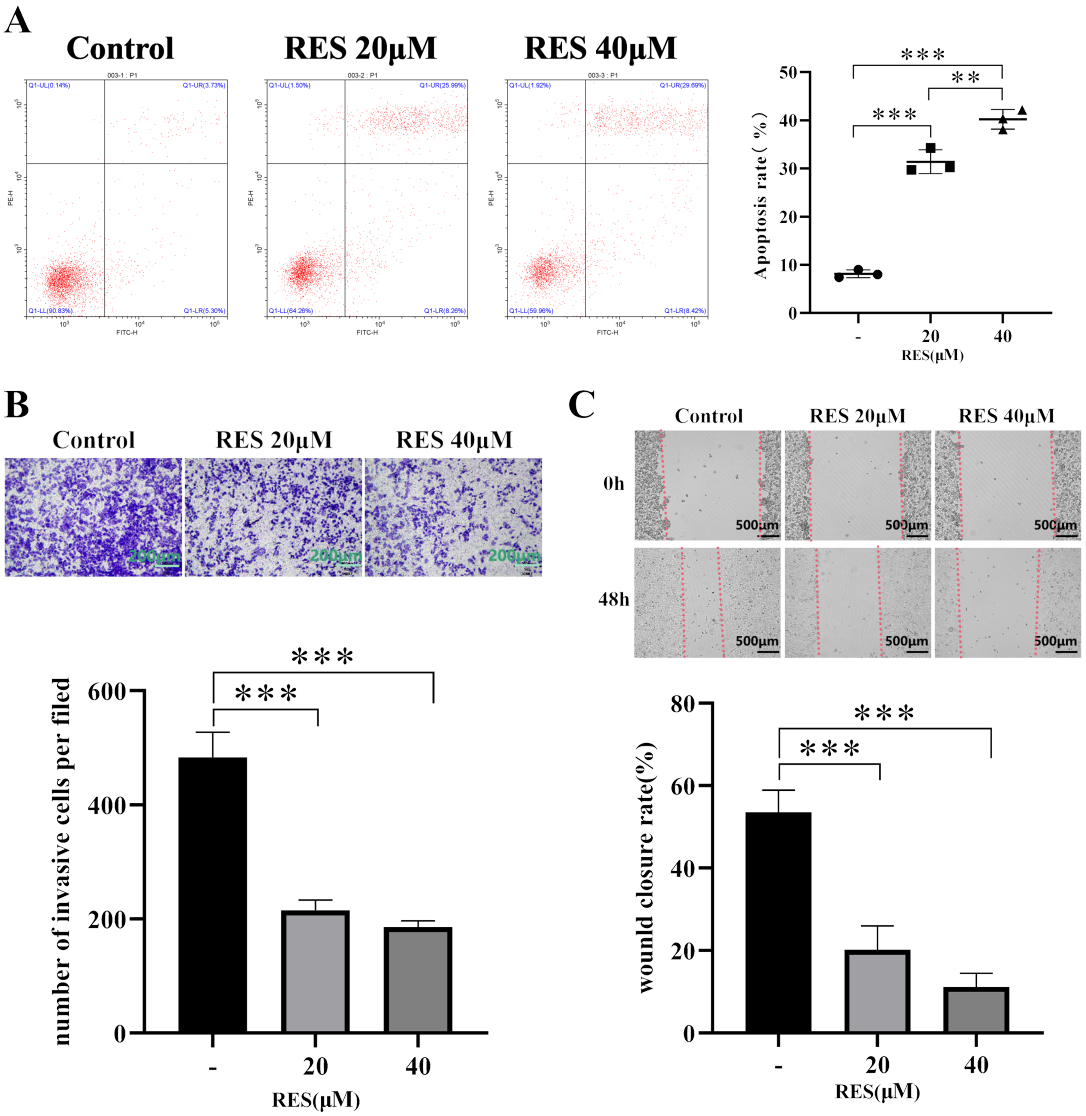

Fig. 2. RES can accelerate A549 cells' apoptosis and inhibit their invasion and migration. Apoptosis (A), invasion (B), and migration (C) of A549 cells following RES treatment (n = 3), scale bar: (B) 200 μm, (C) 500 μm. ** means $p < 0.01$ and *** means $p < 0.001$. The findings are expressed as the mean ± SD.

emerged, indicating a suitable model for subsequent experimentations. At this stage, the size of the tumors was assessed and weighed. After five weeks, tumor volume was computed, and statistical analysis was conducted to compare the tumor growth at both time points. Tumor volume was computed using the formula: V (mm^3) = 1/6 × π × length × $width^2$.

Naked mice were randomly placed into a model group and a RES treatment group (five naked mice for each group). The RES group was administered intraperitoneally with 10 mg/kg of resveratrol, whereas the model group received the same volume of normal saline once daily for 28 days.

After the experiment, the mice were euthanized using a CO_2 small animal euthanasia system (LAT-10-0090, Lab Anim Sci-Tech, Beijing, China).

H&E Staining

The tissue was fixed in 4% paraformaldehyde and subsequently dehydrated, paraffin-embedded, sectioned, and subjected to H&E staining (C0105S, Beyotime, Shanghai, China). The morphological changes in the tumor tissue were observed using a light microscope.

TUNEL Staining

Tumor tissues were fixed, embedded in paraffin, and subsequently sectioned into slices. Terminal deoxynucleotidyl transferase-mediated dUTP-biotin nick end labeling assay (TUNEL) staining was performed using the TUNEL Assay Kit (C1088, Beyotime, Shanghai, China), following the manufacturer's instructions. Finally, the apoptotic rate was assessed employing a fluorescence microscope (BX63, Olympus, Tokyo, Japan).

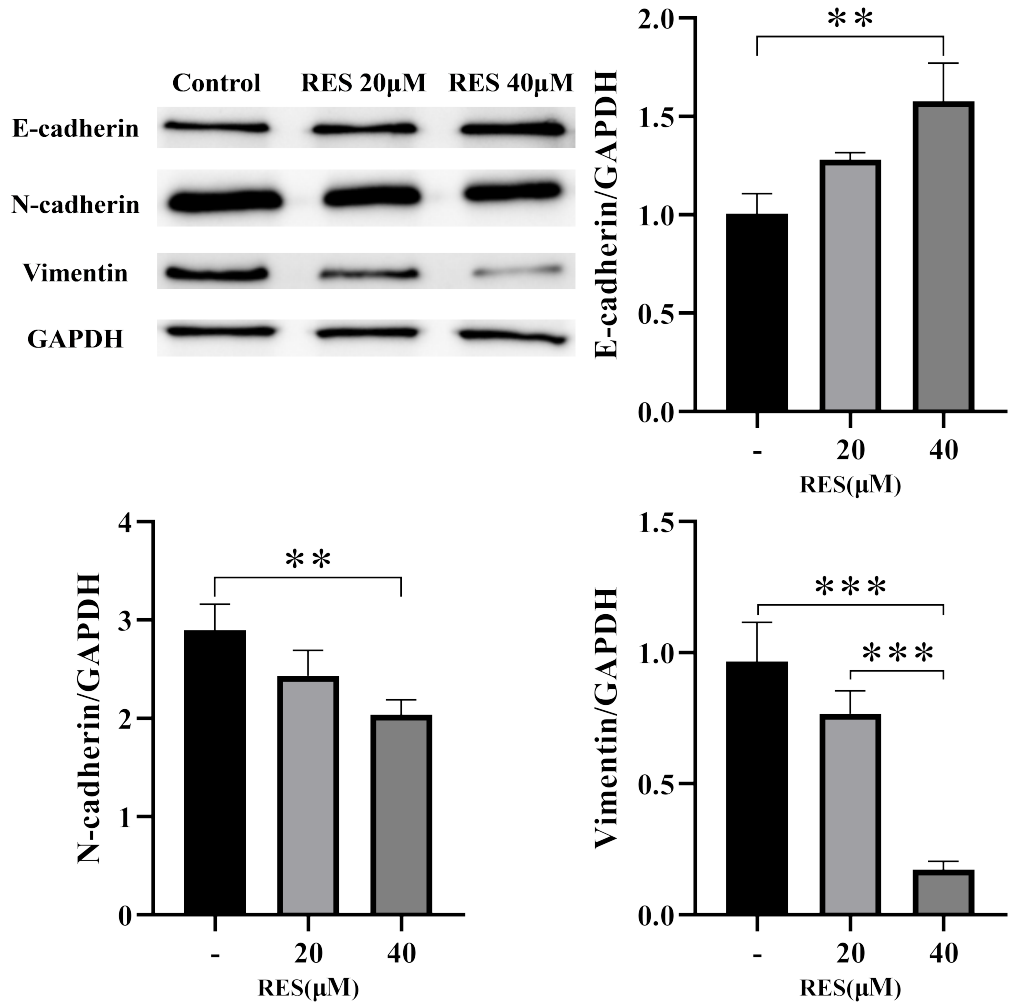

Fig. 3. RES modulates the epithelial-mesenchymal transition (EMT) process in A549 cells. The expression levels of Epithelial-cadherin (E-cadherin), Neuronal-cadherin (N-cadherin), and Vimentin proteins in A549 cells were assessed using Western blotting (WB) analysis following RES treatment (n = 3). ** means $p < 0.01$ and *** means $p < 0.001$. The findings are expressed as mean ± SD. GAPDH, glyceraldehyde 3-phosphate dehydrogenase.

Western Blotting (WB)

The cells supernatant and tissues were lysed utilizing the Radio Immunoprecipitation Assay Lysis (RIPA) buffer (P0013B, Beyotime, Shanghai, China), followed by quantification of the proteins using a Bicinchoninic Acid Assay (BCA) Protein Assay Kit (P0012S, Beyotime, Shanghai, China). The proteins were separated on 12% SDS-PAGE (B7021S, New England Biolabs, Ipswich, MA, USA) and transferred onto PVDF membranes. The membranes were incubated overnight with primary antibodies against Epithelial-cadherin (E-cadherin, 1:500, A3044, ABclonal, Wuhan, China), Neuronal-cadherin (N-cadherin, 1:1000, A3045, ABclonal, Wuhan, China), Vimentin (1:500, A11423, ABclonal, Wuhan, China), Matrix Metalloproteinase-2 (MMP2, 1:1000, A6247, ABclonal, Wuhan, China), and Matrix Metalloproteinase-9 (MMP9, 1:500, A25299, ABclonal, Wuhan, China) at 4 °C. Glyceraldehyde 3-phosphate dehydrogenase (GAPDH, 1:10,000, AC001, ABclonal, Wuhan, China) was utilized as an internal control. The membranes were washed to eliminate the unbound antibodies, and incubated with the HRP Goat Anti-Rabbit IgG (H+L) (1:2000, AS014, ABclonal, Wuhan, China) secondary antibody. The immunoblots were developed, images of the protein bands were captured, and the grayscale values of the protein bands were assessed using ImageJ software (V1.8.0.112, NIH, Madison, WI, USA).

Immunofluorescence Staining

The treated tumor tissues were initially fixed, rinsed, and permeabilized with 0.5% TritonX-100. They were blocked with 10% goat serum at room temperature for 2 hours. After this, the tissues were treated with Inducible Nitric Oxide Synthase (iNOS, 1:20, LS-B12375, LSBio, Seattle, WA, USA), Cluster of Differentiation 206 (CD206, 1:50, bsm-52791R, Bioss Inc., Beijing, China), Lympho-

Journal of
BIOLOGICAL REGULATORS
and Homeostatic Agents

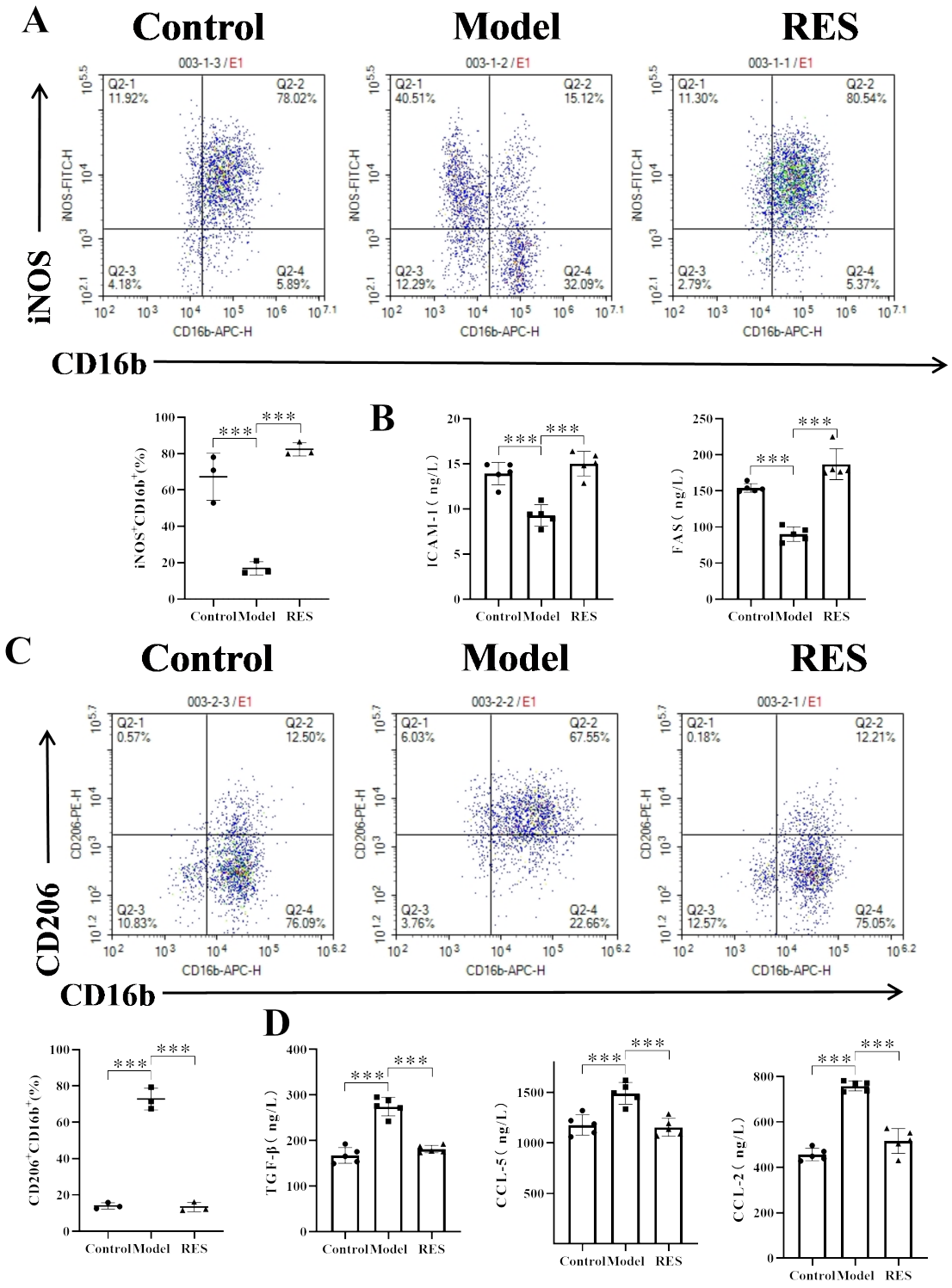

Fig. 4. RES promotes tumor-associated neutrophil (TAN) polarization towards N1. (A) The double positive rate of Inducible Nitric Oxide Synthase (iNOS)$^{+}$, Cluster of Differentiation (CD)16b^{+} of co-cultured A549 cells and neutrophils following RES treatment was determined using FCM (n = 3). (B) The levels of intercellular cell adhesion molecule-1 (ICAM-1) and fatty acid synthase (FAS) associated with N1 TAN phenotype of co-cultured A549 cells and neutrophils after RES treatment were determined utilizing enzyme-linked immunosorbent assay (ELISA) (n = 5). (C) Double positive rate for CD206^{+} CD16b^{+} of co-cultured A549 cells and neutrophils following RES treatment was evaluated using FCM (n = 3). (D) The levels of Transforming Growth Factor-Beta (TGF-β), C-C motif chemokine ligand 5 (CCL-5), and CCL-2 associated with N2 TAN of co-cultured A549 cells and neutrophils following RES treatment were assessed employing ELISA (n = 5). *** means $p < 0.001$. The findings are expressed as the mean ± SD.

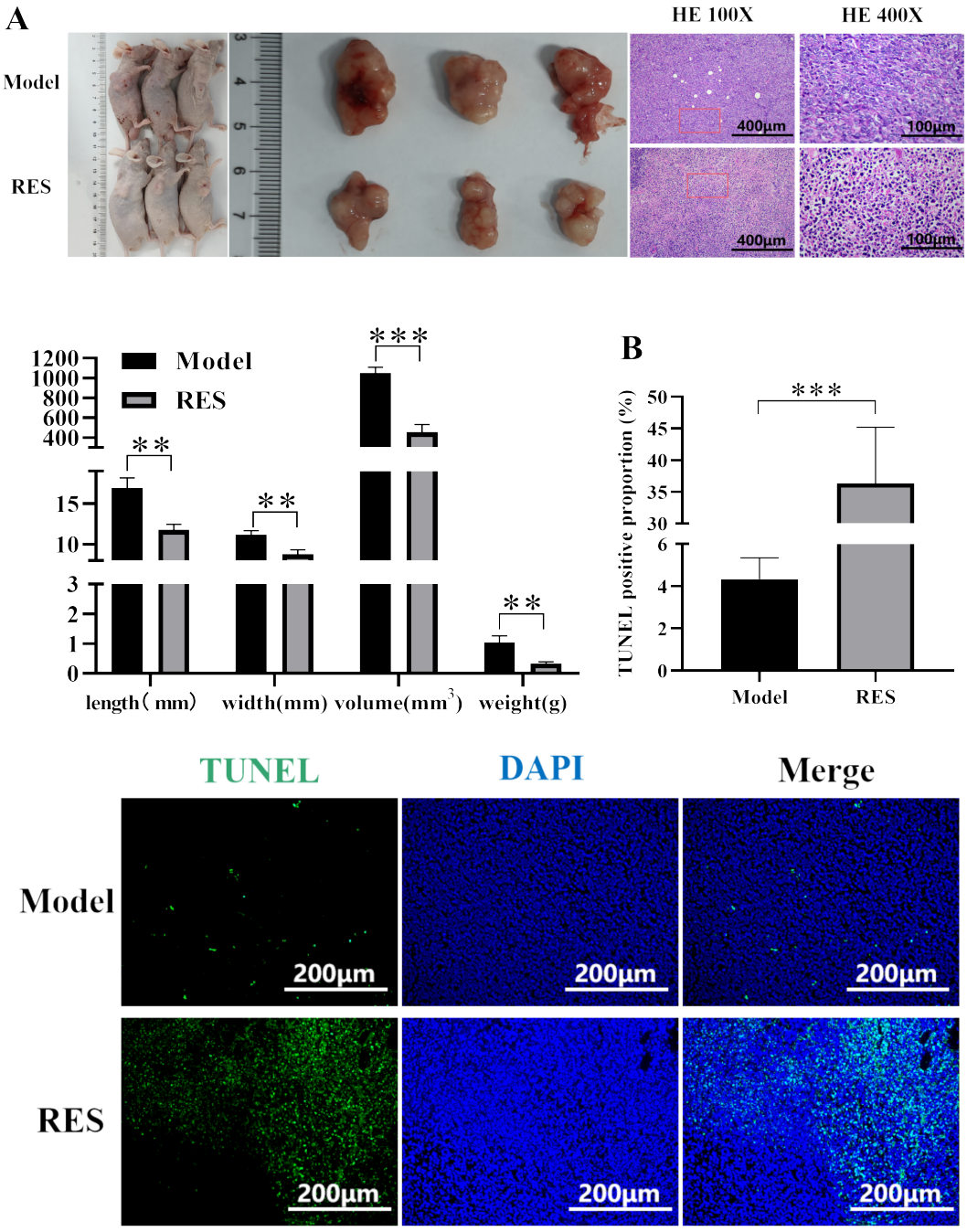

Fig. 5. RES treatment impedes the development of lung tumors and modifies their pathological morphology. Nude mice were inoculated with A549 cells and then administered with RES (the RES group) or normal saline (the model group). (A) The growth of the tumor in the RES group and the Model group (n = 5) and H&E staining (n = 3) (scale bar: 400 μm and 100 μm). (B) Terminal deoxynucleotidyl transferase-mediated dUTP-biotin nick end labeling assay (TUNEL) staining (scale bar: 200 μm) of tumor tissue in the RES and Model groups (n = 3). ** means $p < 0.01$ and *** means $p < 0.001$. The findings are expressed as the mean ± SD. H&E, hematoxylin and eosin.

cyte antigen 6 complex, locus G (Ly6G, 1:50, NB600-1387, Novus Biologicals, Beijing, China) and incubated overnight. The next day, the tissue underwent a PBS wash, followed by dropwise addition of fluorescent FITC Goat Anti-Rabbit IgG (H+L) (1:200, AS011, ABclonal, Wuhan, China), and incubation at room temperature in the dark. After washing, tissue sections were incubated with DAPI staining solution at room temperature for 10 minutes. In the next step, they were washed, mounted with neutral gum, and observed using a fluorescence microscope (BX63, Olympus, Tokyo, Japan).

Journal of
BIOLOGICAL REGULATORS
and Homeostatic Agents

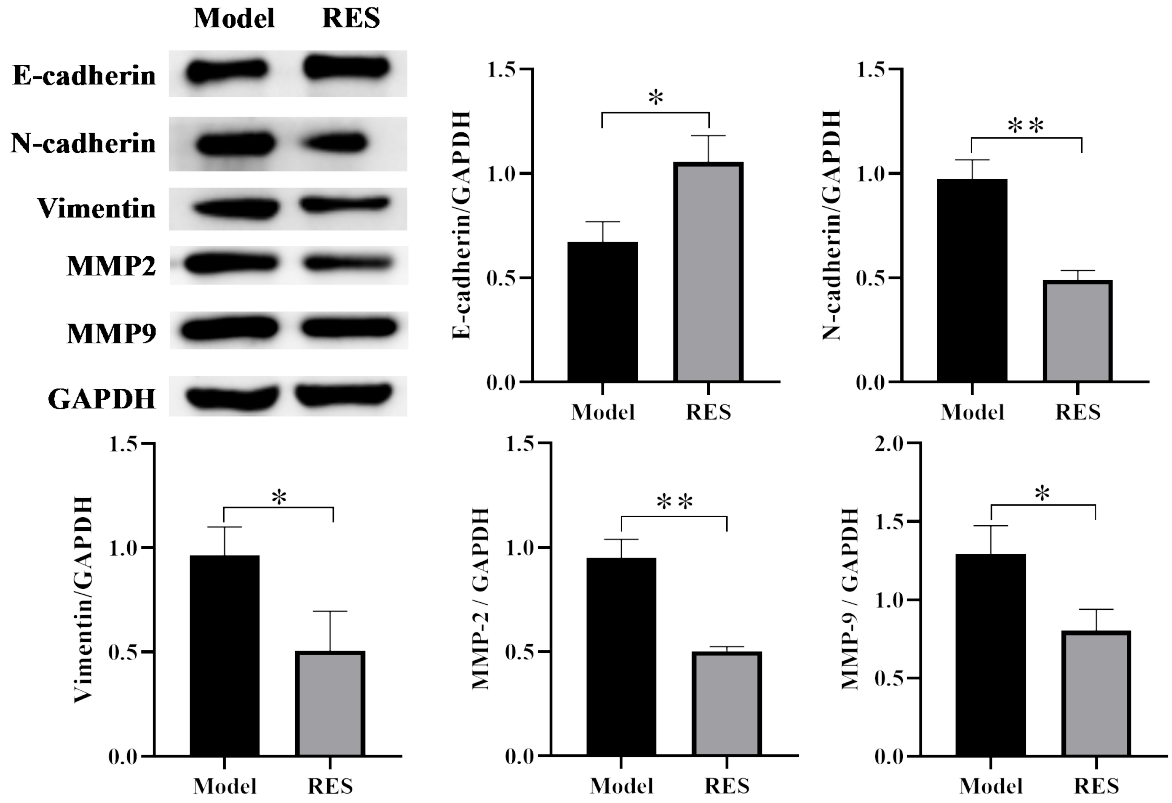

Fig. 6. RES impedes EMT and metastasis of lung cancer cells in tumor-bearing mice. Nude mice were inoculated with A549 cells and then administered with RES (the RES group) or normal saline (the Model group). The expression levels of E-cadherin, N-cadherin, Vimentin, Matrix Metalloproteinase-2 (MMP2), and MMP9 protein in tumor tissues within the RES group and the Model group (n = 3). * $p < 0.05$ and ** $p < 0.01$. The findings are expressed as the mean ± SD.

Enzyme-Linked Immunosorbent Assay (ELISA)

Mouse tumor tissues were extracted and prepared for further analysis. Corresponding ELISA kits were employed to detect Transforming Growth Factor-Beta (TGF-β) (ELH-TGFb1-1, RayBiotech, Beijing, China), C-C motif chemokine ligand 2 (CCL-2) (CKERS-CCL2-145H, Creative Diagnostics, Shanghai, China), CCL-5 (CKERS-CCL5-197H, Creative Diagnostics, Shanghai, China), fatty acid synthase (FAS) (EH0126, Wuhan Fine Biotech Co., Ltd., Wuhan, China), and intercellular cell adhesion molecule-1 (ICAM-1) (EK0370, ScienCell Research Laboratories, San Diego, CA, USA), following the guidelines provided by assay kits.

Statistical Analysis

Statistical analysis was conducted using GraphPad Prism software (V8.0, Dotmatics, Boston, MA, USA). The data were presented as the mean ± standard deviation (SD). Multiple group comparisons were performed using one-way ANOVA. Moreover, the difference between the two groups was assessed using the *t*-test. Furthermore, ImageJ was utilized to evaluate the histological investigation of tumor tissue.

Results

Association of Various RES Dosages with Tumor Proliferation

Initially, A549 lung cancer cells were treated with varying concentrations of RES (0, 5, 10, 20, 40, and 60 μM). Subsequently, CCK-8 reagent was added, followed by evaluation of OD450 values. The RES at a concentration over 10 μM effectively inhibited the proliferation of A549 cells ($p < 0.001$, Fig. 1). It was observed that the inhibitory effects of RES increase with elevation in their dosage. However, when the concentration exceeds 60 μM, it indicates no further increase in its inhibitory effects.

RES Treatment Accelerates A549 Cells' Apoptosis and Inhibits Their Invasion and Migration

Subsequently, we determined the impact of RES on the biological behavior of the A549 cells by treating them with doses of 20 and 40 μM. We observed a significant increase in apoptosis among A549 cells at both 20 μM ($p < 0.001$) and 40 μM concentrations of RES ($p < 0.01$), as shown in Fig. 2A. Furthermore, treatment with 20 μM of RES was significantly associated with a decrease in the invasion and migration of A549 cells, evidenced by a substan-

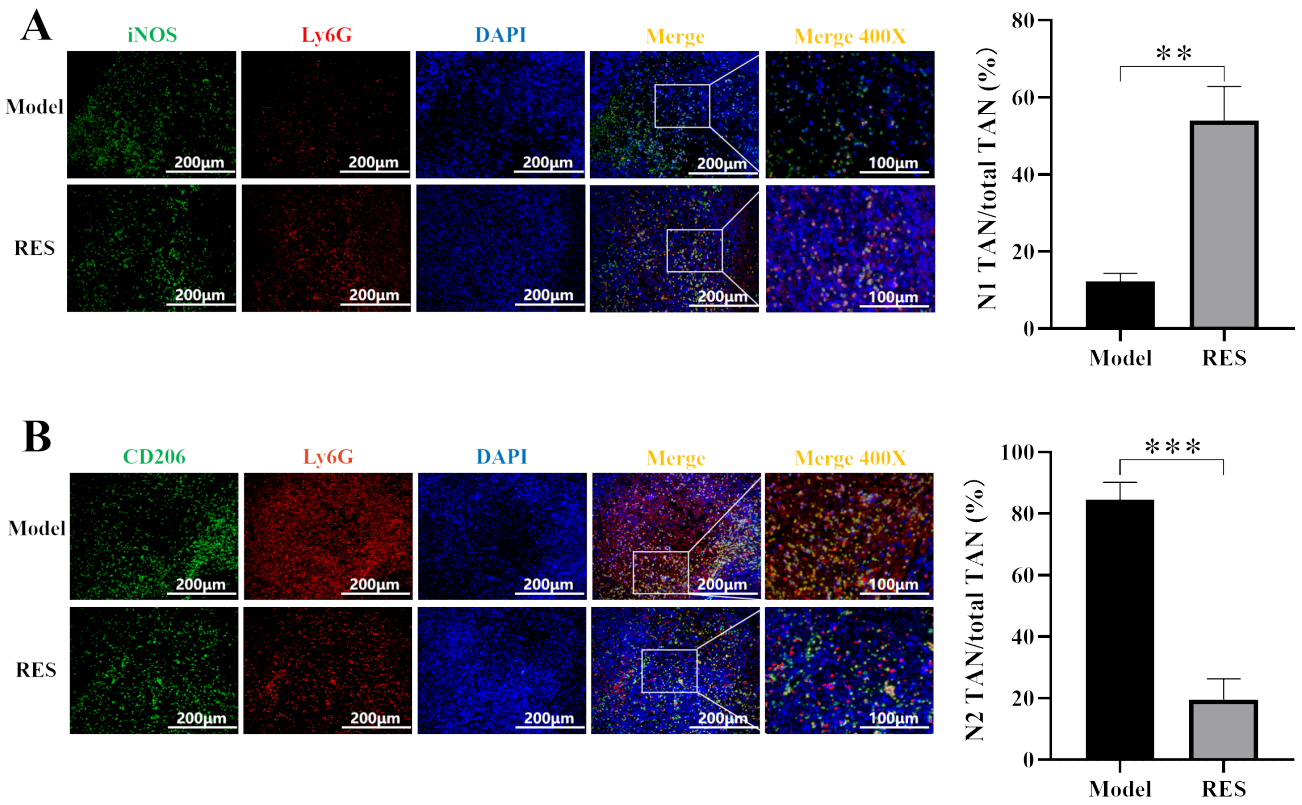

Fig. 7. RES limits TAN N2 polarization and promotes N1 polarization in tumor-bearing mice. Nude mice were inoculated with A549 cells and then administered with RES (the RES group) or normal saline (the Model group). (A,B) The IF staining (A: iNOS: green, Lymphocyte antigen 6 complex, locus G (Ly6G): red, and Merge: yellow) (B: CD206: green, Ly6G: red, and Merge: yellow) of tumor tissue in RES group and Model group (n = 3) (scale bar: 200 μm & 100 μm). ** means $p < 0.01$ and *** means $p < 0.001$. The findings are expressed as the mean ± SD.

tial reduction in the number of invasive cells and the rate of wound healing compared to the control group ($p < 0.001$, Fig. 2B,C).

RES Treatment Modulates the EMT in A549 Cells

We assessed the impact of RES treatment on the expression of epithelial-mesenchymal transition (EMT)-related proteins. As proven in Fig. 3, the administration of 40 μM RES significantly elevated the expression of E-cadherin protein while reducing N-cadherin and Vimentin expression ($p < 0.01$). These findings imply that RES treatment suppresses the mechanism of EMT.

RES Treatment Promotes TAN Polarization towards N1

Healthy human neutrophils were isolated and co-cultured with A549 cells to investigate the precise mechanism underlying the anti-lung cancer impacts of RES. The findings revealed that co-cultivation potentially stimulated the polarization of neutrophils towards the N2 type. The N2 TANs-related chemokines TGF-β, CCL-5, CCL-2, $CD206^+$, and $CD16b^+$ double positive rates were significantly higher in the Model group (co-culture group) ($p < 0.001$), as shown in Fig. 4C,D. However, this N2 polarization was effectively reversed following RES treatment. Furthermore, a significant increase in the double positive rate of ICAM-1, FAS, and $iNOS^+$ $CD16b^+$ was observed in the N1 phenotype, suggesting TAN polarization towards N1 ($p < 0.001$, Fig. 4A–D). These findings indicate that RES enhances TAN N1 polarization while inhibiting TAN N2 polarization.

RES Treatment Suppresses the Development of Lung Tumors and Modifies Their Pathological Morphology

To further explore the anti-tumor efficacy of RES, we established a nude mouse model of subcutaneous tumor implantation, as depicted in Fig. 5A. Our findings demonstrated that RES significantly suppressed tumor development, as evidenced by the considerable reduction in both the volume and mass of tumors in mice following RES treatment ($p < 0.01$). Furthermore, we observed that RES ameliorated the pathological morphology of tumor tissues and boosted apoptosis of tumor cells ($p < 0.001$, Fig. 5A,B).

Journal of
BIOLOGICAL REGULATORS
and Homeostatic Agents

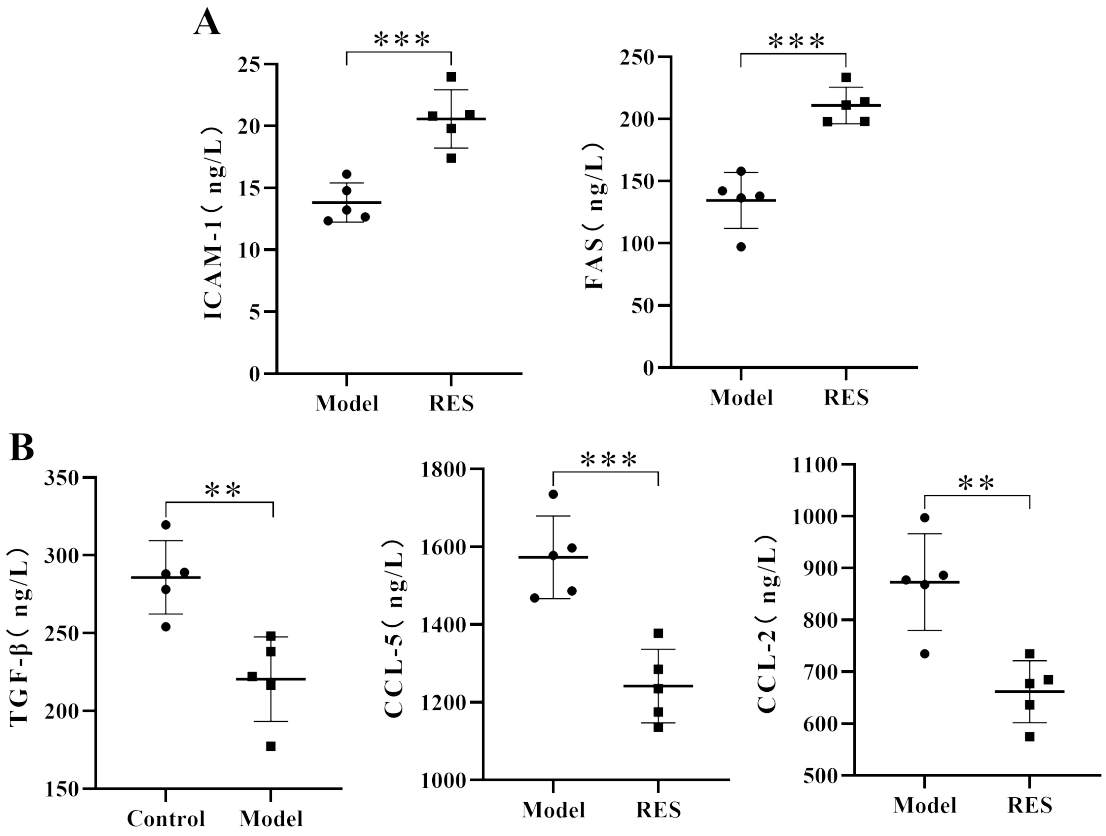

Fig. 8. RES downregulates N2 TAN polarization markers and upregulates N1 TAN polarization markers (n = 5). Nude mice were inoculated with A549 cells and then administered with RES (the RES group) and normal saline (the Model group). (A) The levels of ICAM-1 and FAS associated with N1 TAN phenotype of tumor tissue in the RES group and the Model group. (B) The TGF-β, CCL-5, and CCL-2 levels associated with N2 TAN of tumor tissue in the RES group and the Model group. ** means $p < 0.01$ and *** means $p < 0.001$. The findings are expressed as the mean ± SD.

RES Impedes EMT and Metastasis of Lung Cancer Cells in Tumor-Bearing Mice

Furthermore, we observed that RES significantly restricted EMT in tumor cells, as evidenced by alterations in the expression levels of E-cadherin (upregulated), N-cadherin, and Vimentin protein (downregulated) following RES treatment ($p < 0.05$). Additionally, RES repressed the expressions of MMP2 and MMP9 proteins in tumor tissues ($p < 0.05$). These findings indicate that RES can impede EMT and metastasis in tumor cells (Fig. 6).

RES Limits TAN N2 Polarization and Promotes N1 Polarization in Tumor-Bearing Mice

The polarization state of TAN plays a crucial role in tumor metastasis. As depicted in Fig. 7A,B, the colocalization (Merge) of iNOS and Ly6G increases ($p < 0.01$), whereas the colocalization of CD206 and Ly6G decreases ($p < 0.001$) in the RES group. This demonstrates that RES can limit TAN N2 polarization while promoting TAN N1 polarization, which is favorable for inhibiting tumor metastasis.

RES Downregulates N2 TAN Polarization Markers and Upregulates N1 TAN Polarization Markers

RES treatment significantly elevated ICAM-1 and FAS levels ($p < 0.001$) while lowering TGF-β, CCL-5, and CCL-2 levels ($p < 0.01$), which are vital signaling molecules for N1 and N2 TANs, respectively (Fig. 8).

Discussion

In this study, we utilized A549 cells due to their relatively strong invasion and migration capabilities to investigate the therapeutic effectiveness of RES in lung cancer and elucidate the underlying molecular mechanisms. We observed that RES exerts several impacts on lung cancer, including decreasing lung cancer cell growth, increasing apoptosis, preventing invasion and migration, and modulating the polarization state of TANs.

Initially, we observed that within a specific concentration range, RES effectively suppressed the growth of A549 cells, induced apoptosis, and inhibited invasion and migration. These observations align with earlier research indicating that RES possesses anti-tumor effects. Through

co-culture experiments with A549 cells, we uncovered RES's capability to foster iNOS$^+$ CD16b$^+$ while alleviating CD206$^+$ CD16b$^+$ double positive rate. Similarly, tumor tissue immunofluorescence analysis from RES-treated lung cancer tumor-bearing mice indicated decreased colocalization of CD206 and increased colocalization of iNOS and Ly6G. Among them, CD16b and Ly6G proteins are receptors on the surface of neutrophils [9], and their detection helps identify neutrophils, thus facilitating the analysis of the number and status of neutrophils in lung cancer [4]. iNOS (N1) and CD206 (N2) are critical predictors for distinguishing the polarization of TANs [4]. Furthermore, our *in vivo* and *in vitro* experiments revealed that RES enhances the upregulation of ICAM-1 and FAS while concomitantly downregulating TGF-β, CCL-5, and CCL-2. Neutrophils polarized towards N1 exhibit a pro-inflammatory phenotype, characterized by elevated levels of ICAM-1 [10] and FAS [11]. Findings have demonstrated that elevated levels of ICAM-1 in plasma are associated with prolonged survival and the activation of cytotoxic T cells, thereby enhancing the efficacy of anti-PD-1 therapy [12]. Furthermore, Sato *et al*. [13] reported that the high responsiveness of FasL-induced cell apoptosis depends on FAS expression levels. Additionally, TGF-β secreted by HCC cells activates the ERK1/2 signaling pathway, thereby accelerating the progression of HCC. Moreover, the upregulation of the CLCF1-CXCL6/TGF-β axis demonstrates a considerable correlation with the emergence of "N2" polarized TANs [14]. Chemokines such as CCL-5 and CCL-2 play a crucial role in regulating the migration and directional movement of immune cells [15,16]. In summary, RES can induce a shift in TANs from an N2 to an N1 phenotype. Available evidence suggests that during the initial stages of tumor development, TANs predominantly exhibit an N1 phenotype, exerting anti-tumor effects. However, in the advanced stages of tumor progression, TANs primarily function as an N2 phenotype, thereby promoting tumorigenesis, invasion, and metastasis [17]. This implies that RES may potentially impact lung cancer growth and metastasis by modifying TANs' immunological phenotypes and influencing the TME. However, additional research is required to elucidate the exact molecular mechanisms and signaling pathways underlying this phenomenon.

We further investigated the regulatory effect of RES on the EMT process in lung cancer cells. EMT is closely correlated with immunosuppression and drug resistance, crucial in tumor metastasis [18]. Yun *et al*. [19] found through experiments that in response to $(NH_4)_2SO_4$, N-acetylcysteine (NAC) can inhibit EMT, thereby suppressing the invasion and migration of A549 cells. Our findings suggest that the inhibitory effect of RES may involve the modulation of EMT pathways, providing new insights for a deeper understanding of the anti-tumor mechanisms of RES. Moreover, studies have demonstrated that TGF-β can induce the EMT process [20], and it is also considered one of the markers of the N2 phenotype [21]. Li *et al*. [22] reported a significant interaction between EMT and tumor-associated neutrophils (TANs) in gastric cancer, wherein TANs secrete IL-17a to promote the EMT process. Our experimental findings indicate that RES can inhibit EMT while also influencing the polarization of TANs. In summary, we propose that RES might exert inhibitory effects on EMT in lung cancer by modulating the polarization of TANs.

Although our study provides preliminary insights into the potential mechanisms of RES in lung cancer treatment, there are still some limitations that need to be acknowledged. For instance, while we focused on the effects of RES on TANs and EMT, further research is needed to elucidate the specific immunoregulatory mechanisms and the interaction between TANs and EMT within the lung cancer microenvironment.

Conclusion

This study investigated the mechanism by which RES functions in lung cancer treatment. The findings revealed that RES has the potential to inhibit the growth and metastasis of lung cancer by modulating the polarization state of TANs and influencing the process of EMT. In summary, RES might exert its anti-lung cancer effects by regulating the immunophenotype and polarization of TANs, consequently suppressing EMT. These findings suggest that RES holds promise as a potential therapeutic agent for lung cancer and can target TANs and modulate EMT.

Availability of Data and Materials

Data are available from the corresponding author upon reasonable request.

Author Contributions

GBL contributed to the conception and design of the research study, performed experiments, analyzed and interpreted the data, and drafted the manuscript. HJP performed experiments, analyzed and interpreted the data. SYL contributed to the analysis and interpretation of the data, provided technical support. YPL and NY provided expertise in the field of study, contributed to the interpretation of the data. All authors contributed to editorial changes in the manuscript. All authors read and approved the final manuscript. All authors have participated sufficiently in the work and agreed to be accountable for all aspects of the work.

Ethics Approval and Consent to Participate

All the study participants provided written informed consent, and the study protocol adhered to the principles outlined in the Declaration of Helsinki. Furthermore, the

Journal of
BIOLOGICAL REGULATORS
and Homeostatic Agents

study design was approved by the ethics committee of the First Affiliated Hospital of Guangxi Medical University, China (GXMU2023010). All experimental procedures involving animals were approved by the Animal Experimentation Ethics Committee of the First Affiliated Hospital of Guangxi Medical University, China (GXMUD2023008).

Acknowledgment

Not applicable.

Funding

This research is supported by National Key Clinical Specialty Construction Project (S20210098).

Conflict of Interest

The authors declare no conflict of interest.

References

[1] Zhang Z, Ji Y, Hu N, Yu Q, Zhang X, Li J, *et al*. Ferroptosis-induced anticancer effect of resveratrol with a biomimetic nanodelivery system in colorectal cancer treatment. Asian Journal of Pharmaceutical Sciences. 2022; 17: 751–766.

[2] Chen J, Huang ST, Chen JG, He JH, Lin WM, Huang ZH, *et al*. Resveratrol reduces lactate production and modifies the ovarian cancer immune microenvironment. Neoplasma. 2022; 69: 1129–1137.

[3] Xie C, Liang C, Wang R, Yi K, Zhou X, Li X, *et al*. Resveratrol suppresses lung cancer by targeting cancer stem-like cells and regulating tumor microenvironment. The Journal of Nutritional Biochemistry. 2023; 112: 109211.

[4] Li C, Xu Y, Zhang J, Zhang Y, He W, Ju J, *et al*. The effect of resveratrol, curcumin and quercetin combination on immuno-suppression of tumor microenvironment for breast tumor-bearing mice. Scientific Reports. 2023; 13: 13278.

[5] Que H, Fu Q, Lan T, Tian X, Wei X. Tumor-associated neutrophils and neutrophil-targeted cancer therapies. Biochimica et Biophysica Acta. Reviews on Cancer. 2022; 1877: 188762.

[6] Hu Q, Wang R, Zhang J, Xue Q, Ding B. Tumor-associated neutrophils upregulate PANoptosis to foster an immunosuppressive microenvironment of non-small cell lung cancer. Cancer Immunology, Immunotherapy. 2023; 72: 4293–4308.

[7] Antuamwine BB, Bosnjakovic R, Hofmann-Vega F, Wang X, Theodosiou T, Iliopoulos I, *et al*. N1 versus N2 and PMN-MDSC: A critical appraisal of current concepts on tumor-associated neutrophils and new directions for human oncology. Immunological Reviews. 2023; 314: 250–279.

[8] Chung JYF, Tang PCT, Chan MKK, Xue VW, Huang XR, Ng CSH, *et al*. Smad3 is essential for polarization of tumor-associated neutrophils in non-small cell lung carcinoma. Nature Communications. 2023; 14: 1794.

[9] Shin AE, Tesfagiorgis Y, Larsen F, Derouet M, Zeng PYF, Good HJ, *et al*. F4/80^{+}Ly6C^{high} Macrophages Lead to Cell Plasticity and Cancer Initiation in Colitis. Gastroenterology. 2023; 164: 593–609.e13.

[10] Ohms M, Möller S, Laskay T. An Attempt to Polarize Human Neutrophils Toward N1 and N2 Phenotypes *in vitro*. Frontiers in Immunology. 2020; 11: 532.

[11] Yuan M, Zhu H, Xu J, Zheng Y, Cao X, Liu Q. Tumor-Derived CXCL1 Promotes Lung Cancer Growth via Recruitment of Tumor-Associated Neutrophils. Journal of Immunology Research. 2016; 2016: 6530410.

[12] Lee SH, Kim Y, Jeon BN, Kim G, Sohn J, Yoon Y, *et al*. Intracellular Adhesion Molecule-1 Improves Responsiveness to Immune Checkpoint Inhibitor by Activating CD8^{+} T Cells. Advanced Science. 2023; 10: e2204378.

[13] Sato Y, Yoshino H, Tsuruga E, Kashiwakura I. Fas Ligand Enhances Apoptosis of Human Lung Cancer Cells Cotreated with RIG-I-like Receptor Agonist and Radiation. Current Cancer Drug Targets. 2020; 20: 372–381.

[14] Song M, He J, Pan QZ, Yang J, Zhao J, Zhang YJ, *et al*. Cancer-Associated Fibroblast-Mediated Cellular Crosstalk Supports Hepatocellular Carcinoma Progression. Hepatology. 2021; 73: 1717–1735.

[15] Korbecki J, Kojder K, Simińska D, Bohatyrewicz R, Gutowska I, Chlubek D, *et al*. CC Chemokines in a Tumor: A Review of Pro-Cancer and Anti-Cancer Properties of the Ligands of Receptors CCR1, CCR2, CCR3, and CCR4. International Journal of Molecular Sciences. 2020; 21: 8412.

[16] Ben-Baruch A. The Tumor-Promoting Flow of Cells Into, Within and Out of the Tumor Site: Regulation by the Inflammatory Axis of TNFα and Chemokines. Cancer Microenvironment. 2012; 5: 151–164.

[17] Zhou J, Liu H, Jiang S, Wang W. Role of tumor-associated neutrophils in lung cancer (Review). Oncology Letters. 2022; 25: 2.

[18] Xiao GY, Tan X, Rodriguez BL, Gibbons DL, Wang S, Wu C, *et al*. EMT activates exocytotic Rabs to coordinate invasion and immunosuppression in lung cancer. Proceedings of the National Academy of Sciences of the United States of America. 2023; 120: e2220276120.

[19] Yun Y, Gao R, Yue H, Guo L, Li G, Sang N. Sulfate Aerosols Promote Lung Cancer Metastasis by Epigenetically Regulating the Epithelial-to-Mesenchymal Transition (EMT). Environmental Science & Technology. 2017; 51: 11401–11411.

[20] Kim BN, Ahn DH, Kang N, Yeo CD, Kim YK, Lee KY, *et al*. TGF-β induced EMT and stemness characteristics are associated with epigenetic regulation in lung cancer. Scientific Reports. 2020; 10: 10597.

[21] Schernberg A, Blanchard P, Chargari C, Deutsch E. Neutrophils, a candidate biomarker and target for radiation therapy? Acta Oncologica. 2017; 56: 1522–1530.

[22] Li S, Cong X, Gao H, Lan X, Li Z, Wang W, *et al*. Tumor-associated neutrophils induce EMT by IL-17a to promote migration and invasion in gastric cancer cells. Journal of Experimental & Clinical Cancer Research. 2019; 38: 6.